Compartmental Analysis of Technetium-99m-Teboroxime Kinetics Employing Fast Dynamic SPECT at Rest and Stress

Ping-Chun Chiao, Edward P. Ficaro, Firat Dayanikli, W. Leslie Rogers and Markus Schwaiger

Department of Internal Medicine, Division of Nuclear Medicine, University of Michigan Medical Center, Ann Arbor, Michigan

We have examined the feasibility of compartmental analysis of ^{99m}Tc-teboroxime kinetics in measuring physiological changes in response to adenosine-induced coronary vasodilation. To evaluate the effect of tracer recirculation on ^{99m}Tc-teboroxime kinetics in the myocardium, we also compared compartmental analysis with washout analysis (monoexponential fitting), which does not account for this effect. **Methods:** Eight healthy male volunteers were imaged using fast dynamic SPECT protocols (5 sec per tomographic image) at rest and during adenosine infusion. A two-compartment model was used and compartmental parameters K1 and k2 (characterizing the diffusion of ^{99m}Tc-teboroxime from the blood to the myocardium and from the myocardium to the blood, respectively) were fitted from myocardial time-activity curves and left ventricular input functions. **Results:** Both K1 and washout estimates for the whole left ventricular myocardium changed significantly in response to coronary vasodilation. Mean stress-to-rest (S/R) ratios were almost two times higher for K1 (S/R = 2.7 ± 1.1) than for washout estimates (S/R = 1.5 ± 0.3). Estimation of K1 for all local regions, except the septal wall, is feasible because variations in K1 estimates for all local regions, except the septum during stress, are comparable with those for the global region. **Conclusions:** We conclude that quantitative compartmental analysis of ^{99m}Tc-teboroxime kinetics provides a sensitive indicator for changes in response to adenosine-induced coronary vasodilation.

Key Words: SPECT; technetium-99m teboroxime; cardiac imaging; compartmental modeling

J Nucl Med 1994; 35:1265–1273

Technetium-99m-teboroxime is a neutral lipophilic compound with high myocardial extraction and rapid washout kinetics (*1,2*). Its washout from the myocardium has been shown to correlate with myocardial blood flow in close-chested animal models using SPECT (*2,3*) and planar (*4,5*) imaging techniques, as well as in open-chested animal models using external radiation detectors (*2,6*). Inspired by the rapid washout kinetics of ^{99m}Tc-teboroxime, clinical research activities have been devoted to evaluating and validating fast ^{99m}Tc-teboroxime imaging against conventional ^{201}Tl imaging in the detection of myocardial ischemia and coronary artery disease (*5,7–11*). In addition, several investigators have focused on extracting additional diagnostic information from the washout kinetics of ^{99m}Tc-teboroxime (*7,12*). Potential use of the washout kinetics has also been emphasized and discussed in the literature (*13,14*). However, data acquisition protocols for measuring ^{99m}Tc-teboroxime kinetics and data processing methods for analyzing the kinetics have not been fully explored.

Recently, compartmental modeling, a well established method in PET dynamic data analysis, has been proposed in combination with fast acquisition protocols using three-headed SPECT systems to study ^{99m}Tc-teboroxime kinetics in animal models (*15,16*). By mathematically describing the exchange of radiotracers between the blood and the myocardium, compartmental modeling can be used to characterize not only washout but also washin kinetics of employed radiotracers. By tomographically measuring the organ radiotracer concentration (output), one can determine compartmental parameters (system) using measurements of the blood radiotracer concentration (input). The incorporation of blood radiotracer concentration measurements in compartmental analysis automatically accounts for the effect of recirculating radioactivities following intravenous injection of the tracer. In cardiac studies, the blood radiotracer concentration can be conveniently estimated from a left ventricular region of interest (ROI). It has been shown feasible to obtain the left ventricular input function in dynamic ^{99m}Tc-teboroxime studies using a three-headed SPECT system with 5–10 sec scan duration per tomographic image (*15,17*).

The goal of this investigation was to determine the feasibility of compartmental analysis of ^{99m}Tc-teboroxime kinetics in measuring physiological changes in response to

Received Sept. 27, 1993; revision accepted March 23, 1994.

For correspondence and reprints contact: Ping-Chun Chiao, PhD, The University of Michigan Medical Center, Cyclotron/PET Facility, 3480 Kresge III Bldg., Ann Arbor, MI 48109-0552.

pharmacological vasodilation in normal volunteers. To evaluate the effect of tracer recirculation on ^{99m}Tc-teboroxime kinetics in the myocardium, we also compared compartmental analysis with washout analysis (monoexponential fitting), which does not account for this effect. In addition, we assessed the effects of potential difficulties such as model fitting, attenuation and estimation of local parameters.

METHODS

Study Population

Eight normal volunteers without known risk factors for coronary artery disease were enrolled in the study. Each volunteer had a normal electrocardiogram and a normal physical examination. All of the volunteers were male with an age range of 31 to 58 yr (mean age 46 ± 8 yr). All volunteers were requested to abstain from caffeine and any theophylline-containing medicines at least 24 hr prior to the study.

Imaging Protocol

Each volunteer underwent a resting and an adenosine-induced stress study on separate days. The mean separation time was 59 ± 20 hr. The volunteers were supine during both studies. For the stress study, peripheral intravenous lines were placed in both arms of the patient for the administration of adenosine and ^{99m}Tc-teboroxime. Adenosine was injected over 6 min at 0.140 ml/kg/min using a Harvard pump. Two minutes after the initiation of the adenosine infusion, 25 mCi of ^{99m}Tc-teboroxime in a 3-cc volume was injected over 20 sec using a second Harvard pump. It has been shown, in PET simulation studies, that image-derived input functions for compartmental analysis can be optimized with a 30-sec injection protocol (*18*). Since we analyzed the acquired dynamic data using not only compartmental analysis but also washout analysis, which requires a sharp and consistent input function, we have chosen to use a 20-sec injection protocol with a Harvard pump to ensure that the injection rate was consistent for each patient. For the rest study, 25 mCi of ^{99m}Tc-teboroxime in a 3-cc volume was injected over 20 sec using a Harvard pump. For both studies, dynamic SPECT imaging began at the time of the ^{99m}Tc-teboroxime injection.

Cardiac emission tomography was performed using a three-detector SPECT system (Picker PRISM 3000, Picker Intl., Bedford Heights, OH) fitted with low-energy, high-resolution, parallel hole collimators. A dynamic sequence of 120 × 5.6-sec frames amounting to ~11 min were acquired for each study. Projection data were acquired every 6° over 360° using a 15% energy window centered at 140 keV.

Data Analysis

For parametric analysis, to reduce computation time, projection data from neighboring time frames were combined. We only used the first 19 combined time frames (12 × 11.2 sec, 6 × 33.6 sec and 1 × 67.2 sec), which amounted to 6.7 min in duration. It has been observed that the average time from the termination of adenosine infusion until coronary blood flow returns to basal level is less than 3 min (*19*). Since the adenosine injection stopped 4 min after the start of the ^{99m}Tc-teboroxime injection, using data from the first 6.7 min, we were able to capture the complete vasodilated state. Each combined projection dataset was ramp-reconstructed without smoothing and was resliced to provide short-axis images. We chose not to smooth the images because both compartmental and washout analyses fit a model to the data and can effectively account for noise in the data, and smoothing introduces bias into the parametric analyses.

For clinical diagnosis, projection data from 2 to 6 min postinjection were summed, low-pass filtered, reconstructed and resliced to provide short-axis and horizontal and vertical long-axis slices. The summed short-axis images were also used for delineating myocardial ROIs and the left ventricular ROI, the specifications of which were then superimposed on each short-axis image obtained from the combined data for parametric analysis.

ROIs were placed over the entire annulus-shaped left ventricular myocardium (in each short-axis slice) for global parameter estimation and over the inferior, lateral, anterior and septal walls for local parameter estimation. Myocardial time-activity curves (TACs) were obtained from the average of four midventricular short-axis slices. Blood TACs were obtained from the average of three basal short-axis slices by placing an ROI over the left ventricle in each of these slices.

For compartmental analysis, a two-compartment model was used to characterize the kinetics of myocardial activities. The two-compartment model has two parameters, K1 and k2, which characterize the diffusion of ^{99m}Tc-teboroxime from the blood to the myocardium and from the myocardium to the blood, respectively. In this model, K1 represents the product of blood flow and single-pass extraction fraction (the fraction of the tracer that traverses the capillary membrane and enters the tissue). For washout analysis, a monoexponential function was used to model myocardial TACs from the time to peak to 6.7 min postinjection. In both compartmental and washout analyses, a blood fraction parameter (*20,21*) was introduced to correct for blood count spillover and a nonlinear fit was applied.

Statistical Analysis

Unless explicitly stated, all the hypotheses were tested using the paired-t test. A probability value of <0.05 was considered significant.

RESULTS

Hemodynamic Measurements and Clinical Image Analysis

Dynamic SPECT studies at rest and during adenosine-induced stress were completed in eight normal volunteers. At baseline, systolic and diastolic blood pressure values averaged 128 ± 8 and 75 ± 10 mmHg, and heart rate averaged 72 ± 13 bpm. After adenosine infusion, systolic and diastolic blood pressure values changed to 130 ± 7 and 73 ± 9 mmHg (both changes were not significant), and heart rate to 85 ± 13 bpm ($p < 0.001$). No subject developed an adverse reaction such as chest pain, nausea or bronchospasm after intravenous infusion of adenosine. Visual interpretation of the summed images (from 2 to 6 min postinjection) at rest and during stress did not reveal any perfusion abnormalities in any volunteer.

Time-Activity Curves

Figure 1 shows an example of the myocardial and blood TACs at rest and during stress. The ratio of peak myocardial activity over peak blood activity is higher during stress than at rest, indicating a faster washin process during stress. The curve fit based on the two-compartment model

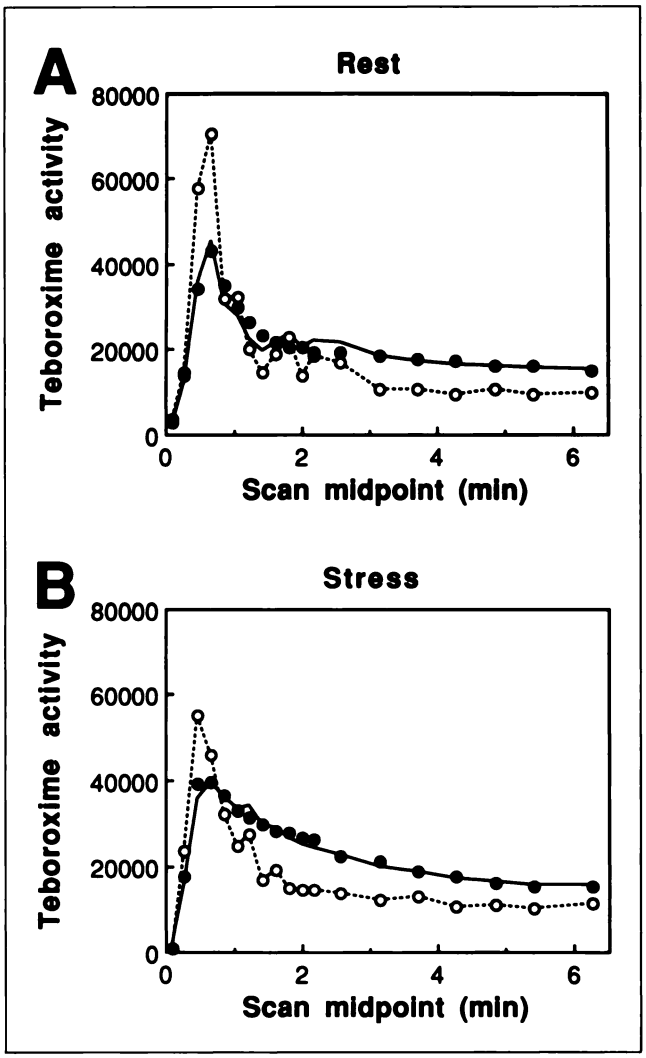

FIGURE 1. An example of the myocardial and plasma TACs at rest (A) and during stress (B). Open circles, dots and solid lines represent plasma TACs, myocardial TACs and fitted myocardial TACs, respectively. The ratio of peak myocardial activity over peak blood activity is higher during stress than at rest, indicating a faster wash-in process during stress. The fit based on the two-compartment model agrees well with the myocardial activity curve in both cases.

agrees well with the myocardial activity curve in both cases.

Estimation of Global Parameters

Table 1 summarizes K1 and washout parameter estimates for the global myocardial ROI. Both K1 and washout estimates showed significant changes in response to adenosine ($p < 0.005$ and $p < 0.005$, respectively). K1 estimates significantly correlated with washout estimates ($r = 0.84$, $p < 0.001$). K1 estimates provided a wider dynamic range of S/R ratios (mean S/R = 2.7 ± 1.1) than washout estimates (mean S/R = 1.5 ± 0.3; $p < 0.01$). However, the percent fraction of the standard deviation (s.d.) relative to the mean S/R ratio was much higher for K1 (40%) than for washout estimates (22%). Subjects 1 and 2 had relatively low K1 S/R ratios, even though their hemodynamic responses to adenosine (rate-pressure products) were significant (both $p < 0.05$). K1 S/R ratios did not significantly correlate with washout S/R ratios.

Estimation of Local Parameters

Although the fitting program ran successfully for global parameter estimation, it occasionally failed to converge to solutions that were in the physiological range for local parameter estimation (especially for the septal wall during stress). When the program failed, the blood fraction estimates usually resulted in values above 0.8 or below 0.25. For this reason, we heuristically set a criterion to omit estimation results that had blood fraction estimates over 0.8 or below 0.25. With this criterion, we included 56 of the total 64 local estimation results.

Figure 2 shows mean local K1 estimates at rest and during stress for both global and local regions. More variations existed in local K1 estimates during stress than at rest. The septal wall during stress had the largest variation in K1 estimates. The standard deviations of K1 estimates for all local regions, except the septum during stress, are comparable with those for the global region. There was a tendency of lower K1 values in the inferior and septal walls as more obviously seen at rest. Figure 3 demonstrates a significant correlation between local K1 and washout esti-

TABLE 1
Global K1 and Washout Estimates from Eight Normal Volunteers

Subject	K1 (ml/g/min)		Washout half-time (min)		K1 Stress/Rest	Washout Rate Stress/Rest
	Rest	Stress	Rest	Stress		
1	1.13	1.35	6.52	5.27	1.19	1.24
2	0.70	0.89	6.24	5.92	1.28	1.05
3	0.71	2.02	8.19	4.06	2.83	2.02
4	0.70	2.57	6.43	5.21	3.70	1.23
5	0.54	2.10	6.18	4.63	3.87	1.33
6	0.78	2.52	6.71	4.00	3.22	1.68
7	1.00	1.93	7.65	4.22	1.94	1.81
8	0.87	2.99	6.81	4.31	3.44	1.58
mean	0.80	2.05	6.84	4.70	2.68	1.49
s.d.	0.19	0.68	0.71	0.69	1.07	0.33

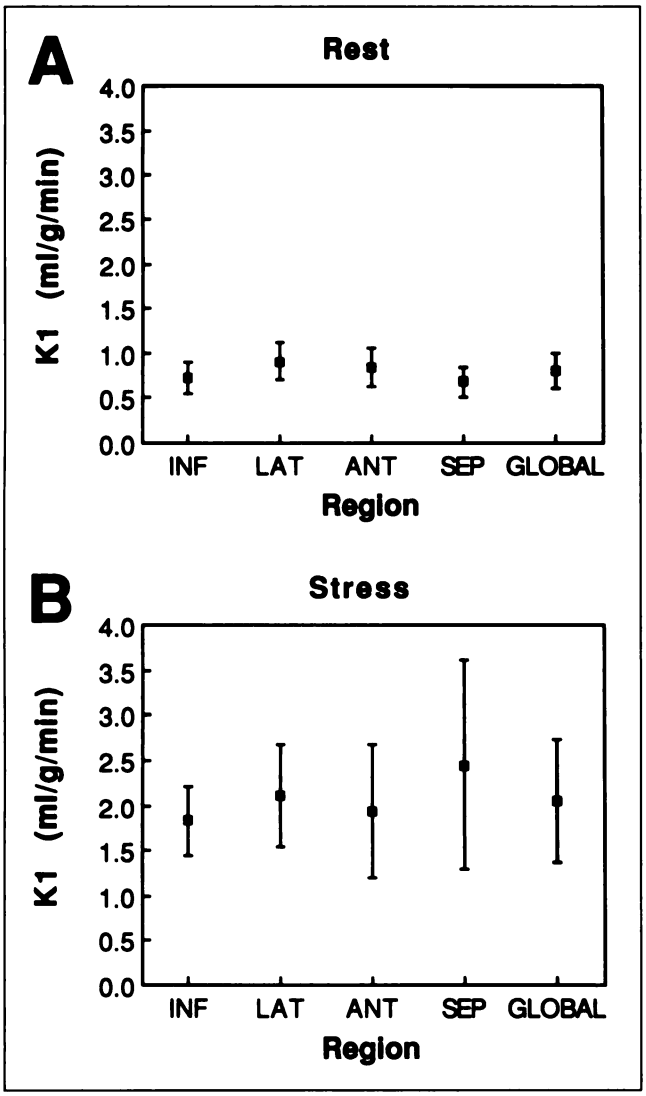

FIGURE 2. Mean K1 estimates at rest (A) and during stress (B) for the global and four local regions: inferior wall (INF), lateral wall (LAT), anterior wall (ANT) and septum (SEP). More variations existed in local K1 estimates during stress than at rest. The septal wall during stress had the highest K1 estimate variation. The variations in K1 estimates for all local regions, except the septum during stress, are comparable with those for the global region. There was a tendency toward lower K1 values in the inferior and septal walls, as more obviously seen at rest.

mates ($r = 0.76$, $p < 0.001$). A significant correlation was also observed between local k2 and washout estimates ($r = 0.68$, $p < 0.001$).

Measuring Changes in Response to Coronary Vasodilation

Figure 4 demonstrates mean K1 and washout S/R ratios for both global and local regions. Similar to global parameter estimation results, K1 analysis gave significantly higher S/R ratios over those derived using washout analysis for all local regions except the septum ($p < 0.05$ for inferior wall, $p < 0.05$ for lateral wall, $p < 0.05$ for anterior wall, and $p = 0.079$ for septal wall). In addition, variations in S/R ratios were much larger for K1 than for washout estimates. Washout S/R ratios were fairly homogeneous throughout the four local regions. K1 S/R ratios for the septal wall had the highest s.d. Similar to results shown in Figure 2, variations in K1 S/R ratios for all local regions, except the septum, are comparable with those for the global region. Local K1 S/R ratios did not correlate with local washout S/R ratios.

Examination of Compartmental Model Fitting

Figure 5 shows the differences between the model fit and measured myocardial activities, called residuals, as a function of time for global parameter estimation in each patient. The residuals were randomly distributed about zero. However, the magnitude of the band of the residuals was not constant as a function of time, showing a similar pattern as typically seen in PET dynamic data analysis (*21*).

Figure 6 demonstrates a significant correlation between local K1 and k2 estimates ($r = 0.95$, $p < 0.001$). K1/k2 ratios, characterizing the distribution volume per unit mass of tissue for a diffusible tracer, did not change significantly ($p > 0.5$ in every case) from rest (1.70 ± 0.35 for inferior wall, 1.72 ± 0.38 for lateral wall, 1.71 ± 0.43 for anterior wall and 1.8 ± 0.55 for septum) to stress (1.77 ± 0.36 for inferior wall, 1.63 ± 0.21 for lateral wall, 1.64 ± 0.3 for anterior wall and 1.84 ± 0.48 for septum).

In Figure 7, although mean blood fractions for the inferior, lateral and anterior walls were not significantly different, the mean blood fraction for the septal wall was significantly higher (Fisher's LSD test).

Attenuation Effects

To assess the effect of attenuation, we combined inferior wall and septal wall counts and anterior wall and lateral wall counts. Inferoseptal wall counts obtained from 2 to 6 min postinjection were normalized to left ventricular counts obtained from the entire study and were significantly lower than anterolateral wall counts ($p < 0.001$). In

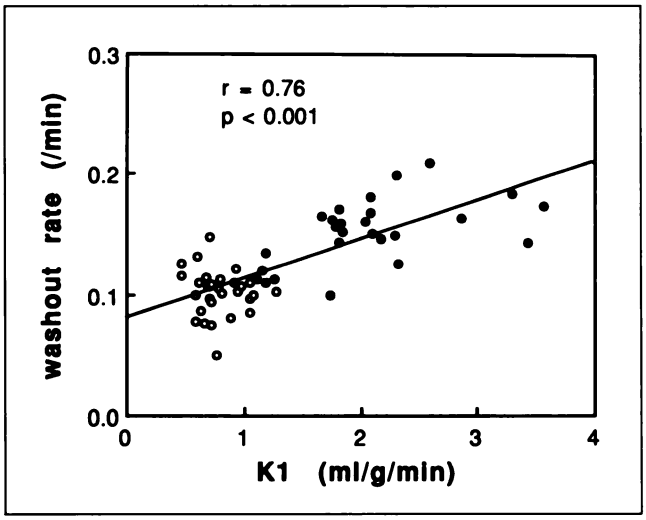

FIGURE 3. Correlation between local K1 and washout estimates. Open circles and dots represent local parameter estimates for all four regions at rest and during stress, respectively.

addition, K1 estimates were significantly lower for the inferoseptal wall than for the anterolateral wall ($p < 0.02$; Wilcoxon signed-rank test). This is most likely due to attenuation effects because both K1 S/R and washout S/R ratios as well as washout estimates for the inferoseptal wall were not significantly different from those for the anterolateral wall.

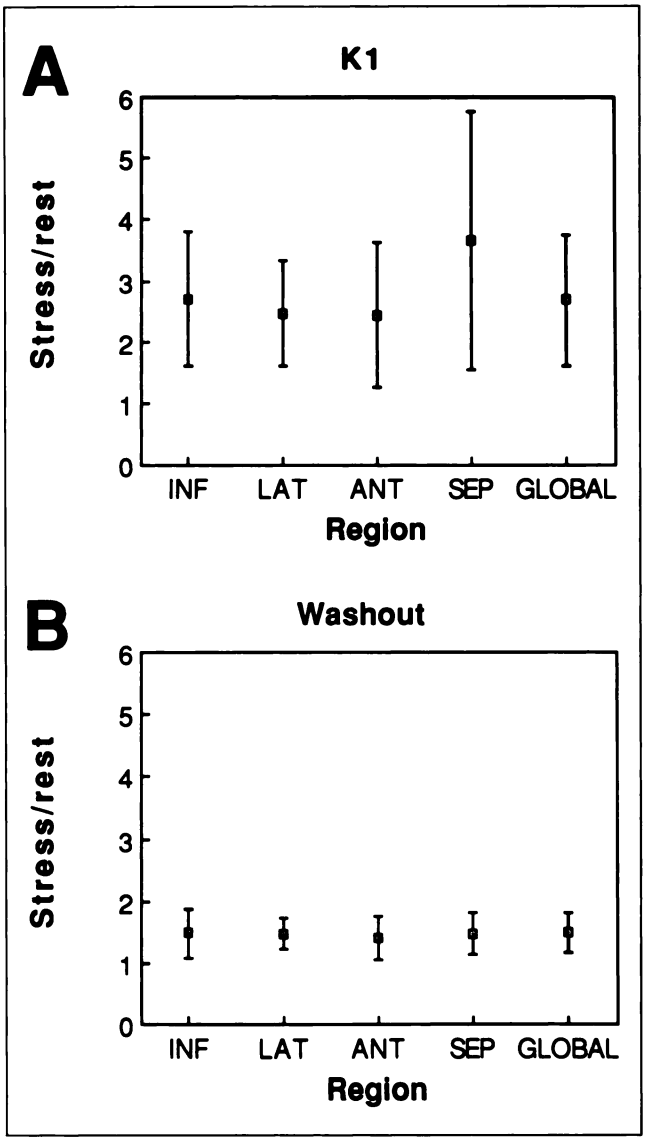

FIGURE 4. Mean K1 (A) and washout (B) S/R ratios. K1 analysis gave significantly higher S/R ratios over those derived using washout analysis for most local regions, except the septum ($p < 0.05$ for inferior wall, $p < 0.05$ for lateral wall, $p < 0.05$ for anterior wall and $p = 0.079$ for septum). In addition, variations in S/R ratios were much larger for K1 than for washout parameters. Washout S/R ratios were fairly homogeneous throughout the four local regions. K1 S/R ratios for the septum had the highest s.d. Global integration of regional counts did not significantly reduce the variations in both K1 and washout S/R ratios.

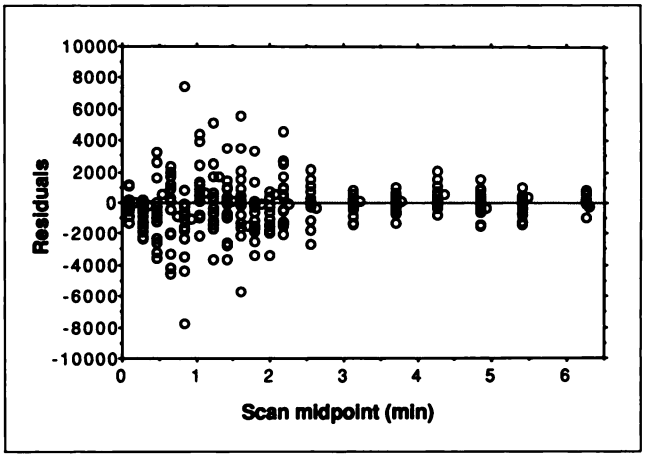

FIGURE 5. Residuals between the model fit and measured myocardial activities as a function of time for global parameter estimation. The data points at each abscissa represent the difference between the model fit and the measured data at that specific time in the study.

DISCUSSION

Compartmental Modeling and Fitting

Compartmental modeling, although powerful and popular in PET, has not been established in SPECT cardiac applications because:

1. Compartmental modeling requires high temporal resolution imaging, which is difficult to achieve with SPECT because it can only provide limited angular sampling at each scan time.
2. Radiotracers with appropriate kinetics have not been available until the recent development of ^{99m}Tc-teboroxime.

With the advances in SPECT technology, scan time can now be reduced to 5 sec per tomographic image with a three-headed SPECT camera. The combination of ^{99m}Tc-teboroxime kinetic characteristics and fast data acquisition protocols provides a unique opportunity for applying compartmental modeling to SPECT cardiac applications.

Technetium-99m-teboroxime was designed to be a diffusible radiotracer, as self-evidenced by its lipophilicity and neutral electrical charge. Several animal studies have also provided evidence for its transport properties. In isolated rabbit hearts, ^{99m}Tc-teboroxime was found to have relatively high myocardial extraction and capillary permeability-surface area product in comparison with ^{201}Tl (*1*). In intact dogs, mean first-pass retention of ^{99m}Tc-teboroxime remained constant over a wide flow range (0.3–7.7 ml/g/min), suggesting that ^{99m}Tc-teboroxime uptake is not diffusion-limited (*2*).

With these transport properties in mind, we chose to characterize ^{99m}Tc-teboroxime kinetics using Kety's two-compartment model with parameters K1 and k2. The model assumes that the exchange of a freely diffusible tracer between the tissue and blood is so rapid and that the tissue and venous outflow concentrations are in equilib-

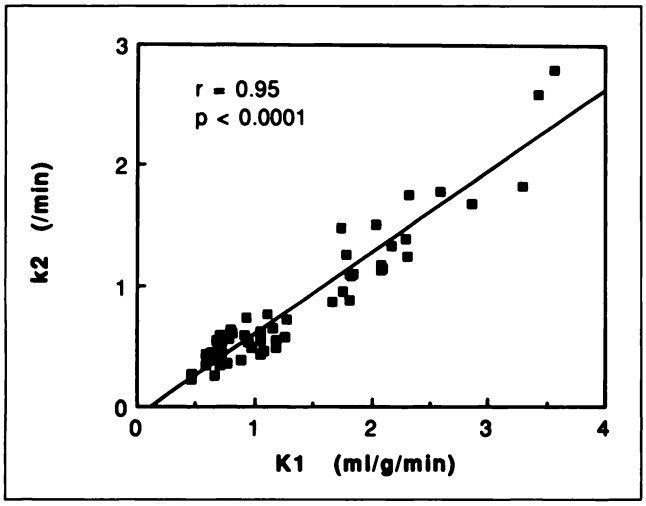

FIGURE 6. Correlation between local K1 and k2 estimates.

rium at any time. With these assumptions, it has been shown (*22,23*) that K1 and k2 are related by a constant term, called partition coefficient or distribution volume.

Human studies (*7,12*), as well as animal studies (*2–6*) have shown that the washout kinetics of ^{99m}Tc-teboroxime are related to myocardial blood flow. In canine models, the relation of ^{99m}Tc-teboroxime retention to blood flow was linear over a wide flow range at 1 min after injection (*24*). This result suggests that the washin kinetics of ^{99m}Tc-teboroxime (partially reflected by the retention within the first minute) are also flow-dependent. Initial compartmental analysis of animal data has demonstrated that K1 estimates correlate significantly with microsphere-determined blood flow (*16*). It is our belief that if the high extraction and diffusible properties of ^{99m}Tc-teboroxime hold in human capillaries then K1, as well as k2 should be closely related to flow. In this investigation, we have focused on K1 estimates because K1 (ml/g/min) has the same unit as blood flow and can be used to compute blood flow if single-pass extraction fraction is known.

The strong correlation between K1 and k2 (Fig. 3) and nearly constant K1/k2 ratios comparing rest with stress indicate that the diffusion of ^{99m}Tc-teboroxime across the blood-tissue boundary is not limited by high blood flow. These results confirm the freely diffusible property of ^{99m}Tc-teboroxime and validate the use of Kety's two-compartment model to estimate blood flow information from ^{99m}Tc-teboroxime kinetics. The relative higher K1 values compared to k2 values suggest a possible binding process for ^{99m}Tc-teboroxime in the myocardium. It is not clear how this binding process may affect the estimation of blood flow information. If the rate of the binding process is not limited by the rate of exchange between the blood and myocardium compartments, then it may be necessary to include one more compartment to account for the existence of the process. It has been shown that ^{99m}Tc-teboroxime tends to bind to plasma proteins and blood cells (*25*). Despite the concerns of the binding of ^{99m}Tc-teboroxime in myocardium and blood, the residuals of the two-compartment fit did not exhibit a problematic pattern, i.e., time-dependent tendency of having more positive or negative residuals.

Whereas estimation of local K1 parameters is feasible for the inferior, lateral and anterior walls, K1 estimation for the septal wall is difficult. We have only analyzed midventricular slices in an attempt not to include the membranous septal area, which does not take up a measurable amount of ^{99m}Tc-teboroxime. However, this area may still contribute a significant volume to the midventricular ROIs due to cardiac motion. Furthermore, septal wall counts are contaminated by count spillover from both left ventricular and right ventricular regions. Therefore, the larger variation in K1 estimates for the septal wall is most likely a result of larger blood fraction (80% as shown in Fig. 7) and, consequently, less signal content in septal wall counts (i.e., only 20% of detected counts are the signal of interest).

Liver uptake of ^{99m}Tc-teboroxime was high and peaked roughly 5 min after injection. Despite the high hepatic uptake, we have not had any difficulties in delineating the inferior wall on the clinical short-axis images (obtained from 2 to 6 min postinjection). In addition, our study did not reveal any significant differences between parameter estimates for the inferior wall and those for the anterior and lateral walls (Figs. 2, 4, and 7). Nonetheless, it is conceivable that the high hepatic uptake can have a significant effect on inferior wall counts through count spillover and scatter. Thus, for more accurate quantitative analysis, it may be necessary to apply scatter correction and to develop methods to minimize count spillover from the liver.

Compartmental Analysis Versus Washout Analysis

Both K1 and washout estimates changed significantly in response to stress (Table 1 and Fig. 4). Although K1 esti-

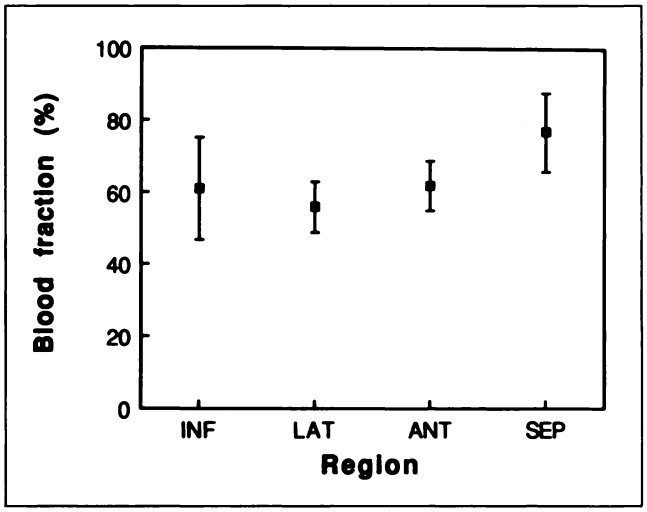

FIGURE 7. Mean blood fraction estimates for four regions: inferior wall (INF), lateral wall (LAT), anterior wall (ANT) and septal wall (SEP). Mean blood fractions for inferior, lateral and anterior walls were not significantly different; the mean blood fraction for the septal wall was significantly higher (Fisher's LSD test).

mates were more sensitive to the coronary vasodilation, they provided S/R ratios with larger variations (Table 1 and Fig. 4). These larger variations can be attributed to two sources, namely, counting noise and intersubject variability.

Counting noise results in noisy input functions and myocardial TACs. Since compartmental analysis inherently performs "deconvolution" of myocardial activities from the influence of input function and automatically accounts for recirculating activities, the accuracy of K1 estimates is not only directly affected by noisy myocardial TACs, but also vulnerable to noisy input functions.

Intersubject variability may be due mainly to differences in individual's response to adenosine (*26*). Even in PET ^{13}N-ammonia myocardial blood flow studies, a large variation in K1 S/R ratios (4.3 ± 1.6; s.d. relative to mean = 37%) has been observed using adenosine (*26*). Although intersubject variability can directly affect both K1 S/R and washout S/R ratios, it may only be observed from estimated K1 S/R ratios, which are more sensitive in reflecting this variability.

The significant correlation (Fig. 3) between K1 and washout estimates is mainly due to an overall trend of higher values of both estimates in vasodilated states because this correlation was not significant in data obtained at either rest or stress alone. In addition, there was no significant correlation between K1 and washout S/R ratios. However, these results do not necessarily suggest that K1 and washout estimates may convey vastly different diagnostic information. The combination of the large variation in K1 estimates and less sensitivity of washout estimates can easily mask any correlation between the two estimates.

Quantification of Myocardial Blood Flow—Next Step

We have shown that it is feasible to estimate not only global but also local K1 parameters. A more challenging question ahead is how to compute blood flow in units of ml/g/min from K1. In other words, following the success of PET (*21,27*), can we quantify myocardial blood flow using SPECT?

Quantification of myocardial blood flow has provided valuable insights in various disease states. Several conditions where coronary angiography did not reveal large-vessel disease, such as syndrome X (*28*), cardiac transplantation (*29*), hypertrophic cardiomyopathy (*30*) and hypertension (*31,32*), have been characterized by abnormal coronary flow reserve. Application of quantitative blood flow measurements could uncover pathophysiology in similar circumstances where there is a global reduction in myocardial blood flow. Regional quantification of myocardial blood flow may have the greatest clinical impact. Especially in selecting patients with severe impairments of coronary flow or flow reserve for invasive procedures such as coronary angiography. Application of quantitative techniques has previously disclosed the efficacy of therapeutic invasive procedures, such as percutaneous transluminal coronary angioplasty (*33*). Thus, noninvasive measurements of myocardial blood flow using dynamic SPECT imaging at rest and following pharmacological vasodilation would be an important clinical tool in diagnostic clinical cardiology.

It is well known that SPECT is an order of magnitude lower in counting sensitivity than PET. This lower sensitivity results in more noisy myocardial TACs and left-ventricular input functions. Therefore, it is essential to develop more robust methods for analyzing SPECT dynamic data. Potential methods include a weighting scheme to account for noisy input functions (*34*) and a model-based method for joint estimation of compartmental parameters, myocardial boundaries and left ventricular input functions directly from projection data (*35*).

Whereas PET has well developed attenuation correction schemes that are routinely used, accurate attenuation correction methods for SPECT are still at their early stage of development. As shown in our results, attenuation significantly affects estimation of local K1 parameters and needs to be corrected. A promising method is being developed, which has been implemented on three-headed SPECT with an external transmission source (*36,37*).

As mentioned above, K1 is related to blood flow and single-pass extraction fraction. It has been shown that single-pass extraction fraction of ^{99m}Tc-teboroxime decreases as flow increases in isolated rabbit hearts (*1*). Further investigations are needed to examine the relation between single-pass extraction fraction of ^{99m}Tc-teboroxime and myocardial blood flow in humans.

It will be both instructive and important to evaluate the performance of quantitative dynamic SPECT analysis against PET results. The development of flow agents labeled with the positron emitter ^{94m}Tc has made such evaluation studies possible (*38*). These studies will be very useful for refining SPECT technology for quantitative studies and for transferring PET experience to SPECT applications.

Study Limitations

The goal of this investigation was to determine the feasibility of compartmental analysis of ^{99m}Tc-teboroxime kinetics in measuring physiological changes in response to coronary vasodilation. We made no attempt to evaluate the diagnostic performance of compartmental analysis against other diagnostic imaging modalities such as angiography. The comparison of K1 analysis with washout analysis was only intended to demonstrate that the inherent correction for tracer recirculation using K1 analysis improves the dynamic range of K1 estimates in response to coronary vasodilation. Since the sample size was relatively small and no gold standard was used in this investigation, we were limited in concluding the diagnostic meaning of the K1 S/R ratio in each individual. For instance, it is beyond the scope of this investigation to conclude why Subjects 1 (41 yr) and 2 (55 yr) had relatively low K1 S/R ratios despite significant hemodynamic responses to adenosine and absence of heart disease.

Because of the relatively small sample size, we cannot conclude that intersubject variability dominates the variations in K1 estimates, and, therefore, do not rule out the possibility that counting noise is also a major cause. We did not use arterial blood measurements, which can potentially provide more accurate input function estimates. Without arterial blood measurements for comparison or more robust methods for analysis, we must question the use of noisy left ventricular input functions. Further investigations are required to determine how much variation in K1 estimates can be reduced by using more accurate input function estimates or more robust analysis methods so that the estimates will be more reproducible.

The "coronary flow reserve" of 2.7 measured by K1 S/R ratios in this investigation is lower than the expected values of 4 to 5 as have been observed using PET (*21,26*) and coronary Doppler catheter (*19,39*). It is very likely (based on animal results) (*1*) that the single-pass extraction of ^{99m}Tc-teboroxime in the human heart is nonlinearly related to blood flow. Since single-pass extraction was not included in the analysis, K1 values may underestimate vasodilated blood flow, resulting in lower values of "coronary flow reserve."

CONCLUSION

Compartmental analysis of ^{99m}Tc-teboroxime kinetics provides a sensitive indicator for changes in response to adenosine-induced coronary vasodilation. The inherent correction for recirculating ^{99m}Tc-teboroxime using compartmental analysis improves the dynamic range of K1 estimates over washout estimates in response to adenosine. K1 estimation for all local regions, except the septal wall, is feasible. Accurate estimation of local K1 parameters requires attenuation correction. Further investigations are required to determine the exact cause of the large variations in K1 estimates.

ACKNOWLEDGMENTS

The authors wish to thank Robert J. Ackermann, Steven Pitt, Lisa A. Cotton and Kathy Stafford for technical assistance. This work was supported by the National Institutes of Health grant 5RO1 HL41047; Department of Energy grant DE-FG02-90ER61091; funds from Ohio Imaging of Picker International, Bedford Heights, OH; and funds from Squibb Diagnostics, Princeton, NJ.

REFERENCES

1. Leppo JA, Meerdink DJ. Comparative myocardial extraction of two technetium-labeled BATO derivatives (SQ30217, SQ32014) and thallium. *J Nucl Med* 1990;31:67–74.
2. Stewart RE, Schwaiger M, Hutchins GD, et al. Myocardial clearance kinetics of technetium-99m-SQ30217: a marker of regional myocardial blood flow. *J Nucl Med* 1990;31:1183–1190.
3. Li QS, Solot G, Frank TL, Wagner HJ, Becker LC. Tomographic myocardial perfusion imaging with technetium-99m-teboroxime at rest and after dipyridamole. *J Nucl Med* 1991;32:1968–1976.
4. Stewart RE, Heyl B, O'Rourke RA, Blumhardt R, Miller DD. Demonstration of differential post-stenotic myocardial technetium-99m-teboroxime clearance kinetics after experimental ischemia and hyperemic stress [Editorial]. *J Nucl Med* 1991;32:2000–2008.
5. Gray WA, Gewirtz H. Comparison of ^{99m}Tc-teboroxime with thallium for myocardial imaging in the presence of a coronary artery stenosis. *Circulation* 1991;84:1796–1807.
6. Johnson G, Glover DK, Hebert CB, Okada RD. Early myocardial clearance kinetics of technetium-99m-teboroxime differentiate normal and flow-restricted canine myocardium at rest. *J Nucl Med* 1993;34:630–636.
7. Seldin DW, Johnson LL, Blood DK, et al. Myocardial perfusion imaging with technetium-99m SQ30217: comparison with thallium-201 and coronary anatomy. *J Nucl Med* 1989;30:312–319.
8. Hendel RC, McSherry B, Karimeddini M, Leppo JA. Diagnostic value of a new myocardial perfusion agent, teboroxime (SQ 30217), utilizing a rapid planar imaging protocol: preliminary results [corrected and republished with original paging, article originally printed in *J Am Coll Cardiol* 1990 Oct;16: 855–861]. *J Am Coll Cardiol* 1990;16:855–861.
9. Fleming RM. Detecting coronary artery disease using SPECT imaging: a comparison of thallium-201 and teboroxime. *Am J Physiol Imaging* 1992;7: 20–23.
10. Taillefer R, Lambert R, Essiambre R, Phaneuf DC, Leveille J. Comparison between thallium-201, technetium-99m-sestamibi and technetium-99m-teboroxime planar myocardial perfusion imaging in detection of coronary artery disease. *J Nucl Med* 1992;33:1091–1098.
11. Dahlberg ST, Weinstein H, Hendel RC, McSherry B, Leppo JA. Planar myocardial perfusion imaging with technetium-99m-teboroxime: comparison by vascular territory with thallium-201 and coronary angiography. *J Nucl Med* 1992;33:1783–1788.
12. Drane WE, Decker M, Strickland P, Tineo A, Zmuda S. Measurement of regional myocardial perfusion using Tc-99m-teboroxime (Cardiotec) and dynamic SPECT [Abstract]. *J Nucl Med* 1989;30:1744.
13. Gewirtz H. Differential myocardial washout of technetium-99m-teboroxime: mechanism and significance [Editorial]. *J Nucl Med* 1991;32:2009–2011.
14. Nunn AD. Is there additional useful information in the myocardial washout characteristics of teboroxime [Editorial]? *J Nucl Med* 1991;32:1988–1991.
15. Smith AM, Gullberg GT, Datz FL, Christian PE. Kinetic modeling of teboroxime using dynamic SPECT imaging [Abstract]. *J Nucl Med* 1992; 33:878–879.
16. Lien DC, Araujo LI, Budinger T, Alavi A. Quantification of myocardial blood flow can be obtained with technetium-99m teboroxime and fast dynamic SPECT scanning [Abstract]. *J Am Coll Cardiol* 1993;21:376A.
17. Budinger T, Araujo L, Ranger N, et al. Dynamic SPECT feasibility studies [Abstract]. *J Nucl Med* 1991;32:955.
18. Raylman RR, Caraher JM, Hutchins GD. Sampling requirements for dynamic cardiac PET studies using image-derived input functions. *J Nucl Med* 1993;34:440–447.
19. Wilson RF, Wyche K, Christensen BV, Zimmer S, Laxson DD. Effects of adenosine on human coronary arterial circulation [Editorial]. *Circulation* 1990;82:1595–1606.
20. Herrero P, Markham J, Bergmann SR. Quantitation of myocardial blood flow with H2 15O and positron emission tomography: assessment and error analysis of a mathematical approach. *J Comput Assist Tomogr* 1989;13:862–873.
21. Hutchins GD, Schwaiger M, Rosenspire KC, Krivokapich J, Schelbert H, Kuhl DE. Noninvasive quantification of regional blood flow in the human heart using N-13 ammonia and dynamic positron emission tomographic imaging. *J Am Coll Cardiol* 1990;15:1032–1042.
22. Kety SS. Theory of blood-tissue exchange and its application to measurement of blood flow. *Methods Med Res* 1960;8:223–236.
23. Kety SS. Measurement of local blood flow by the exchange of an inert, diffusible substance. *Methods Med Res* 1960;8:228–236.
24. Beanlands R, Muzik O, Nguyen N, Petry N, Schwaiger M. The relationship between myocardial retention of technetium-99m-teboroxime and myocardial blood flow [Editorial]. *J Am Coll Cardiol* 1992;20:712–719.
25. Rumsey WL, Rosenspire KC, Nunn AD. Myocardial extraction of teboroxime: effects of teboroxime interaction with blood. *J Nucl Med* 1992;33:94–101.
26. Chan SY, Brunken RC, Czernin J, et al. Comparison of maximal myocardial blood flow during adenosine infusion with that of intravenous dipyridamole in normal men. *J Am Coll Cardiol* 1992;20:979–985.
27. Bergmann SR, Herrero P, Markham J, Weinheimer CJ, Walsh MN. Noninvasive quantitation of myocardial blood flow in human subjects with oxygen-15-labeled water and positron emission tomography. *J Am Coll Cardiol* 1989;14:639–652.
28. Camici PG, Lorenzoni R, Gistri R. Regional coronary vasodilator reserve in syndrome X [Abstract]. *Circulation* 1991;82:III-479.
29. Krivokapich J, Stevenson LW, Kobashigawa J, Huang SC, Schelbert HR.

Quantification of absolute myocardial perfusion at rest and during exercise with positron emission tomography after human cardiac transplantation. *J Am Coll Cardiol* 1991;18:512–517.
30. Camici P, Chiriatti G, Lorenzoni R, Bellina RC, Gistri R, Italiani G. Coronary vasodilation is impaired in both hypertrophied and nonhypertrophied myocardium of patients with hypertrophic cardiomyopathy: a study with nitrogen-13 ammonia and positron emission tomography. *J Am Coll Cardiol* 1991;17:879–886.
31. Opherk D, Mall G, Zebe H, et al. Reduction of coronary reserve: a mechanism for angina pectoris in patients with arterial hypertension and normal coronary arteries. *Circulation* 1984;69:1–7.
32. Brush JJ, Faxon DP, Salmon S, Jacobs AK, Ryan TJ. Abnormal endothelium-dependent coronary vasomotion in hypertensive patients [Editorial]. *J Am Coll Cardiol* 1992;19:809–815.
33. Walsh M, Geltman E, Steele R, et al. Augmented myocardial perfusion reserve after coronary angioplasty quantified by positron emission tomography with $H_2^{15}O$. *J Am Coll Cardiol* 1990;15:119–127.
34. Huesman RH, Mazoyer BM. Kinetic data analysis with a noisy input function. *Phys Med Biol* 1987;32:1569–1579.
35. Chiao P, Rogers WL, Clinthorne NH, Fessler JA, Hero AO. Model-based estimation for dynamic cardiac studies using ECT. *IEEE Trans Med Imag* 1994: in press.
36. Tung CH, Gullberg GT, Zeng GL, Christian PE, Datz FL, Morgan HT. Nonuniform attenuation correction using simultaneous transmission and emission converging tomography. *IEEE Trans Nucl Sci* 1992;39:1134–1143.
37. Ficaro EP, Fessler JA, Rogers WL, Schwaiger M. Comparison of Am-241 and Tc-99m as transmission sources for the attenuation correction of Tl-201 SPECT imaging of the heart. *J Nucl Med* 1994;35:652–663.
38. Nickles RJ, Nunn AD, Stone CK, Christian BT. Technetium-94m-teboroxime: synthesis, dosimetry and initial PET imaging studies. *J Nucl Med* 1993;34:1058–1066.
39. McGinn AL, White CW, Wilson RF. Interstudy variability of coronary flow reserve. Influence of heart rate, arterial pressure, and ventricular preload [Editorial]. *Circulation* 1990;81:1319–1330.